Article

Unraveling the Water-Mediated Proton Conduction Mechanism along the Surface of Graphene Oxide

Le Shi,* Zhixuan Ying, Ao Xu, and Yonghong Cheng
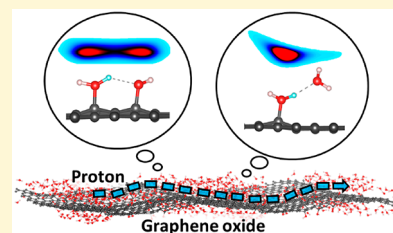
Read Online

ACCESS | 📊 Metrics & More | 📖 Article Recommendations | 🆂🆸 Supporting Information

ABSTRACT: The proton conduction capability of graphene oxide (GO) sheets opened up a new avenue for the design of high-performance solid-state electrolytes, which is urgently needed in areas such as fuel cells and flow batteries. However, the proton conduction mechanism of GO sheets is still unclear, impeding the optimization and further utilization of GO-based proton-conducting electrolytes. In this work, we systematically investigate the proton conduction behavior on the surface of GO sheets with water molecules involved. We find that both epoxide and hydroxyl functional groups can effectively attract water molecules onto the surface of GO sheets to form a dense hydrogen-bonding network. Protons can hop between adjacent as well as nonadjacent hydroxyl functional groups with low energy barriers through the hydrogen-bonding network. On the other hand, the proton conduction capability of epoxide functional groups is relatively low, and spontaneous proton conduction can rarely be observed. Our work suggests that increasing the content of hydroxyl functional groups can lead to a higher proton conductivity of GO sheets.

1. INTRODUCTION

The emergence of two-dimensional (2D) materials opened up a new avenue for the design of the separation membrane. By the drilling of pores on 2D materials[1−3] or the utilization of the intrinsic pores formed by the electron clouds of 2D crystals,[4−6] selective mass transport can be achieved. Another way to realize molecular sieving is restacking exfoliated 2D materials. By tuning of the interlayer spacing of 2D materials, the layer-stacked membrane can be applied in areas such as wastewater treatment, desalination, gas separation, batteries, and so on.[7−9] Graphene oxide (GO) is one of the most popular candidates for the construction of the layer-stacked membrane due to its tunable physicochemical properties and easy preparation.[10] Joshi et al.[11] demonstrated that when immersed in water, micrometer-thick GO laminates can effectively block all solutes with hydrated radii larger than 4.5 Å. Zhou et al.[12] showed that water permeation through the GO membrane could be controlled via changing the electric field. By introducing interlaminar short-chain molecular bridges[13] or cations,[14] the interlayer spacing of GO membranes can be precisely manipulated, and the membrane stability can be improved.

In 2013, Hayami et al.[15] reported that the hydrophilic functional groups of GO (−O−, −OH, −COOH) could attract protons and form a hydrogen-bonding network with adsorbed water molecules. Protons can propagate through the hydrogen-bonding network with an activation energy barrier of 0.284 eV, making GO a new candidate for solid-state proton-conducting electrolytes. The proton-conducting GO nano-sheets have wide range applications in areas such as fuel cells,[16−18] electrolysis,[19] capacitors,[20] and so on. By the introducion of sulfate ions into the GO interlayers, the proton conduction capability of GO could be further improved.[21,22]
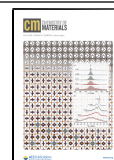
It is now widely agreed that the hydrogen-bonding network formed between the hydrophilic functional groups of GO and adsorbed water molecules can facilitate proton conduction,[23,24] while the detailed proton propagation mechanism is still unclear. Hatakeyama et al.[25] proposed that epoxide functional groups are the major contributor to efficient proton transport. They found that when blocking epoxide groups using ethylenediamine (EDA), the proton conductivity of GO would be significantly decreased. However, Jiang et al.[26] argued that modification of GO with EDA would inevitably neutralize protons associated with the GO/water interface, which may also decrease the proton conductivity. They found that after HCl treatment, the protonation effect of EDA blocked GO can be recovered.

In this work, we comprehensively investigated the detailed proton conduction mechanism on the basal plane of GO by performing extensive reactive force field molecular dynamics (ReaxFF MD) simulations.[27−29] The recently developed CHON-2017 force field[30,31] was employed to characterize the Grotthuss proton-hopping process accurately. Our MD simulations found that both epoxide and hydroxyl functional groups can effectively attract water molecules onto the surface of GO sheets to form a hydrogen-bonding network. Instead of forming hydronium ions with the adsorbed water molecules,

protons tend to bond with the epoxide or hydroxyl functional groups on the surface of GO sheets. Protons can hop between adjacent epoxide functional groups with a moderate energy barrier of 0.21 eV. In comparison, the energy barrier for water-mediated proton conduction between nonadjacent epoxide functional groups is higher than 0.42 eV, which can barely occur at room temperature. On the other hand, the proton-hopping process between adjacent hydroxyl functional groups is nearly barrierless (E_a = 0.016 eV), and the energy barrier for water-mediated proton conduction between nonadjacent hydroxyl functional groups is about 0.12−0.14 eV. The low energy barriers make proton conduction between both adjacent and nonadjacent hydroxyl functional groups feasible at room temperature and can contribute to a good proton conductivity. Our work clarified the detailed water-mediated proton conduction mechanism along the surface of GO sheets and shed light on the future design of GO-based proton-conducting solid-state electrolytes.

2. COMPUTATIONAL METHODOLOGY

All MD simulations were performed using the LAMMPS[32,33] software package. The CHON-2017_weak ReaxFF force field parameters[30,31] were used to capture the Grotthuss proton-hopping process, which has been widely adopted to study the proton/hydroxide transportation behavior.[27,28,34] Detailed validation of the CHON-2017_weak force field has been carried out in our previous work.[43] For all of the MD simulations, the time step was set to be 0.25 fs. A Nosé−Hoover chain thermostat was employed, and the temperature-damping constant was set to be 100 fs for the NVT simulations. For MD simulations calculating detailed proton-hopping energy barriers, the trajectories were recorded every 1 MD step, and for other simulations, the trajectories were recorded every 100 MD steps.

The atomic structure of single-cell graphene was taken from our previous density functional theory (DFT) work[6] as shown in Figure S1. Afterward, 21 × 12 and 8 × 4 supercells were generated to construct the 5.17 × 5.13 nm^2 and 1.97 × 1.71 nm^2 graphene sheets. It is now widely accepted that the surface oxygen functional groups of graphene oxide mainly contribute to the lateral proton conduction capability, and protons can change from the conduction path in one layer to another through nanopores.[25] In our previous work,[3,35] we have investigated the proton conduction capability of graphene nanopores with different kinds of terminations. Therefore, in this work, we concentrate on the lateral proton conduction mechanism along the basal plane of GO. The detailed preparation processes of GO models are elaborated in Figures S2 and S3.

As GO sheets fluctuate during the MD simulations, the distance between the oxygen atom in the water molecule and its nearest carbon atom in GO sheets was defined as the distance between a water molecule and the GO sheets. The water density distribution as a function of distance to GO sheets was calculated as

$$\rho(z) = \frac{M \sum_{i=1}^{N_{frame}} n_i}{N_A A B \Delta z N_{frame}} \tag{1}$$

where M is the mass for 1 mol of water, N_{frame} is the number of frames, n_i is the number of water molecules found inside the slice at frame i, N_A is the Avogadro constant, A and B are the cell dimensions in the x and y directions, which are 5.17 and

5.13 nm in our case, and Δz is set to be 0.2 Å. The spatial distribution of adsorbed water molecules was visualized by calculating the water density based on the hexagonal graphene grid. For each adsorbed water molecule with a distance to GO sheets smaller than 5 Å, its (x, y) position was defined as the initial (x_0, y_0) position of its nearest carbon atom in the GO sheets before the MD simulations. The water density at each grid point was calculated as

$$\rho(x, y) = \frac{M \sum_{i=1}^{N_{frame}} n_i}{N_A A_{hex} Z N_{frame}} \tag{2}$$

where A_{hex} is the area of a hexagonal grid, and Z is set to be 5 Å. In all the calculations involving water density, both sides of the GO sheets were considered. The coverage of adsorbed water molecules was calculated as

$$\text{Coverage} = \frac{N_{nonzero}}{N_{all}} \times 100\% \tag{3}$$

where $N_{nonzero}$ is the number of hexagonal grids with nonzero adsorbed water density, and N_{all} is the number of all hexagonal grids.

To track the proton trajectories, we analyzed the coordination number of each oxygen atom. If one oxygen atom bonds with three hydrogen atoms, we will identify it as the hydronium ion. For GO sheets covered by epoxide functional groups, if one oxygen atom bonds with one/two carbon atom(s) and one hydrogen atom, we will identify it as the epoxide functional group that carries the proton. For GO sheets covered by hydroxyl functional groups, if one oxygen atom bonds with one carbon atom and two hydrogen atoms, we will identify it as the hydroxyl functional group that carries the proton. The C−O bond length threshold was set to be 2.0 Å, and the H−O bond length threshold was set to be 1.35 Å. It is worth noting that in some of our MD simulations, the oxygen functional groups are not stable and may react with water molecules or desorb from the graphene sheets. During all the MD simulations, the state of the oxygen functional groups was monitored. Once the oxygen functional groups desorb from the GO sheets or react with water molecules, the simulation would be terminated, and new structures containing randomly attached oxygen functional groups would be generated. The calculation of proton-hopping energy barriers requires long-time simulation, and the atomic trajectories need to be recorded every step. To enhance the system stability and reduce memory cost, we employed smaller simulation cells (1.97 × 1.71 nm^2).

3. RESULTS AND DISCUSSION

3.1. Water Adsorption Behavior on the Surface of GO Sheets.

It is widely accepted that epoxide and hydroxyl functional groups are the dominant functionalities on the basal plane of GO sheets.[10,36] To clarify the detailed proton conduction capability of these two kinds of functional groups, GO sheets covered by pure epoxide or hydroxyl functional groups were modeled separately. The atomic structures of GO were constructed based on a 5.17 × 5.13 nm^2 graphene sheet. Epoxide or hydroxyl functional groups were added onto both sides of the graphene sheet randomly following the previous report[37] until the oxygen content reached 10, 20, and 30 wt %, respectively. The resulted GO sheets were labeled as E10, E20, E30 and H10, H20, H30 for the GO sheets containing 10, 20, and 30 wt % epoxide or hydroxyl functional groups,

respectively. For each kind of oxygen functional group with specific content, three different GO structures were constructed and studied.

To clarify the interaction between GO/graphene and water, the prepared GO sheets and pure graphene were put into a $5.17 \times 5.13 \times 5.00$ nm^3 cubic box containing randomly distributed water molecules. Water weight ratio (H$_2$O/GO) ranges from 10% to 50% were considered, which correspond to different humidity conditions. The estimated relationship between the water weight ratio and relative humidity from experimental results[38] are listed in Table S1. The systems first went through 500 ps ReaxFF MD simulations in the NVT ensemble (T = 300 K) for equilibration. Afterward, we analyzed the water distribution by collecting data from another 1 ns ReaxFF MD simulation in the NVT ensemble (T = 300 K). Figure 1a shows the atomic geometry of pristine graphene
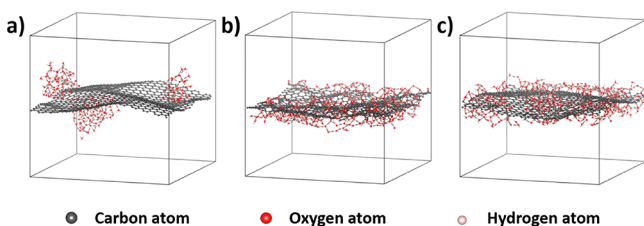

Figure 1. Atomic geometries of graphene and GO in 30% water weight ratio condition: (a) pristine graphene (201 water molecules), (b) E20 GO sheet (241 water molecules), and (c) H20 GO sheet (244 water molecules).

in 30% water weight ratio condition[38] after MD simulations. It can be found that water molecules tend to cluster on the surface of graphene and exhibit a contact angle larger than 90°, which agree well with experimental observations.[39] Results for different water weight ratio conditions vary slightly. The water density distribution as a function of distance to the graphene sheet in different water weight ratio conditions can be found in Figure S4. Figures 1b and 1c show the atomic geometries of one of the E20 and H20 GO sheets in 30% water weight ratio condition after MD simulations. We can see that the appearance of oxygen functional groups significantly changes the water adsorption behavior. For GO sheets covered by either epoxide or hydroxyl functional groups, water molecules tend to uniformly adsorb onto the surface of GO sheets and form a dense hydrogen-bonding network.

The water density distributions as a function of distance to E10, E20, E30 and H10, H20, H30 GO sheets in different water weight ratio conditions are shown in Figures S5 and S6. The water densities were calculated by averaging data from the three different atomic geometries containing the same oxygen content. It can be found that for either epoxide or hydroxyl functional groups, the first density peak of adsorbed water molecules appears at a distance of 3 Å away from the GO sheets. Both the content of oxygen functional groups and water weight ratio influence the water density distribution. Figure 2a shows the peak water density as a function of water weight ratio for different GO sheets. Generally, larger water weight ratio corresponds to higher peak density. For hydroxyl functional groups with the same water weight ratio, more functional groups can attract more water molecules onto the GO surface, which corresponds to higher peak density, while for epoxide functional groups, when the content of functional groups reaches 20 wt %, the water adsorption will become saturated. A further increase in functional groups will not lead to higher peak density. It is widely reported that the local water density can be quite different from the bulk value at the water/2D material interfaces. For example, the local water density can reach higher than 3.0 g/cm^3 on the surface of graphene and h-BN.[40,41] The oxygen functional groups of GO can form hydrogen bonds with water molecules, and it is not surprising that water molecules tend to aggregate on the GO surface, which can result in a local water density higher than the bulk value.

To better understand the interaction between functional groups and water molecules, we visualized the spatial distribution of adsorbed water molecules on the surfaces of GO sheets in 30% water weight ratio condition, as shown in Figure 3. The spatial distribution of adsorbed water on GO sheets in 10%−50% water weight ratio conditions can be found in Figures S7−S12. It can be seen that water molecules tend to aggregate around oxygen functional groups. As the content of the oxygen functional group increases, the distribution of adsorbed water molecules will become more uniform. Figure 2b shows the coverage of adsorbed water molecules as a function of water weight ratio for different GO sheets, where the coverage was defined as the ratio of nonzero adsorbed water density area. Larger water weight ratio corresponds to higher coverage. For both epoxide and hydroxyl functional groups, the coverages for the oxygen content of 20 and 30 wt % show little difference when water weight ratio is larger than 30%, indicating that 20 wt % oxygen functional groups are
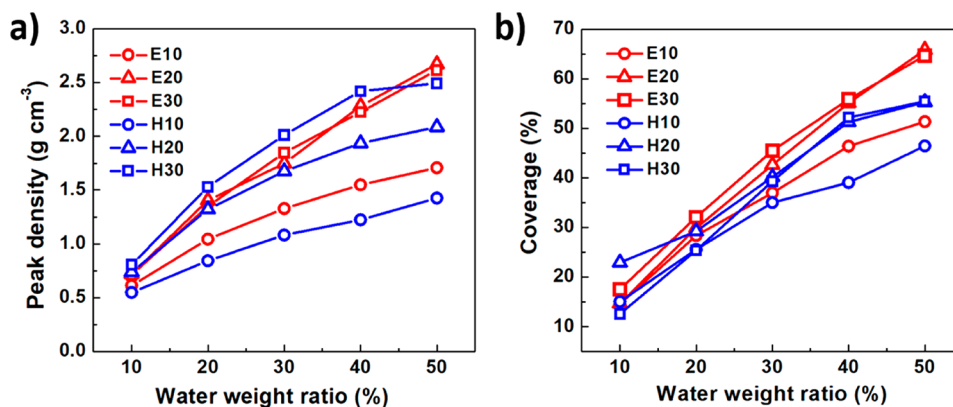

Figure 2. Averaged (a) peak water density and (b) water coverage as a function of water weight ratio for different GO sheets.
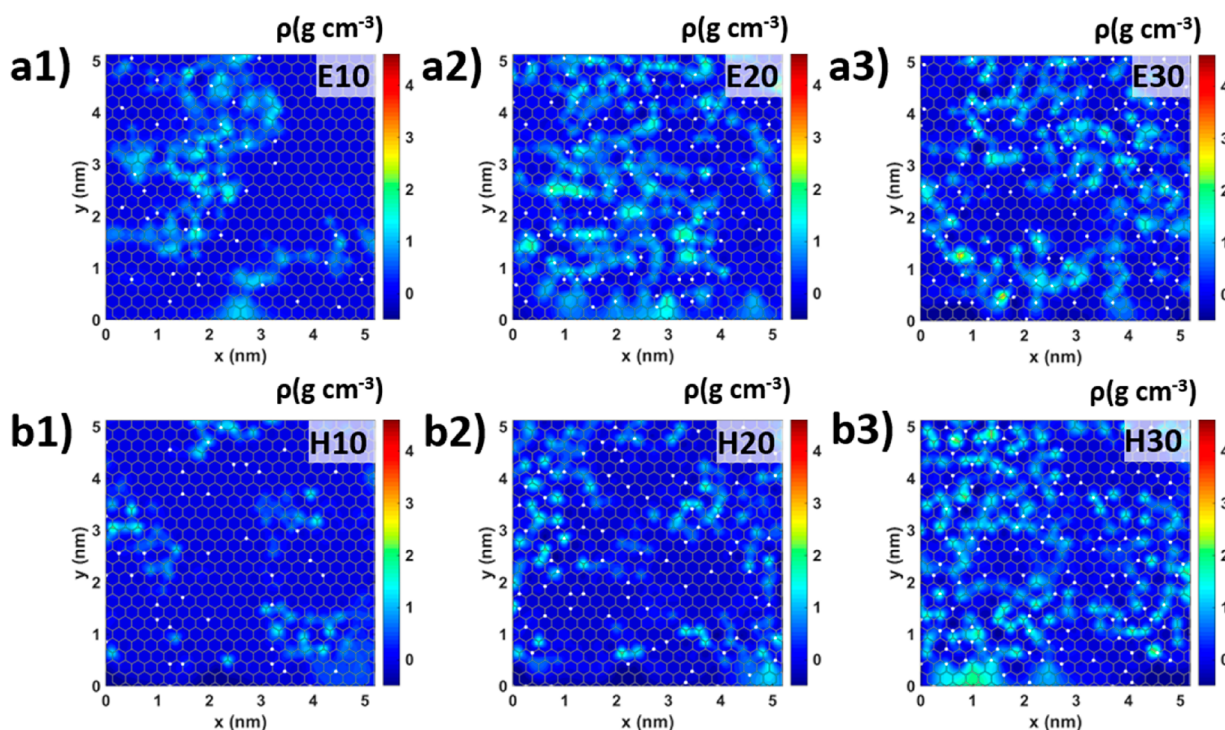
Figure 3. Spatial distribution of adsorbed water molecules on the surface of GO sheets containing different kinds and amounts of functional groups in 30% water weight ratio condition. The gray hexagonal mesh represents the graphene sheet, and the white dots represent oxygen functional groups.
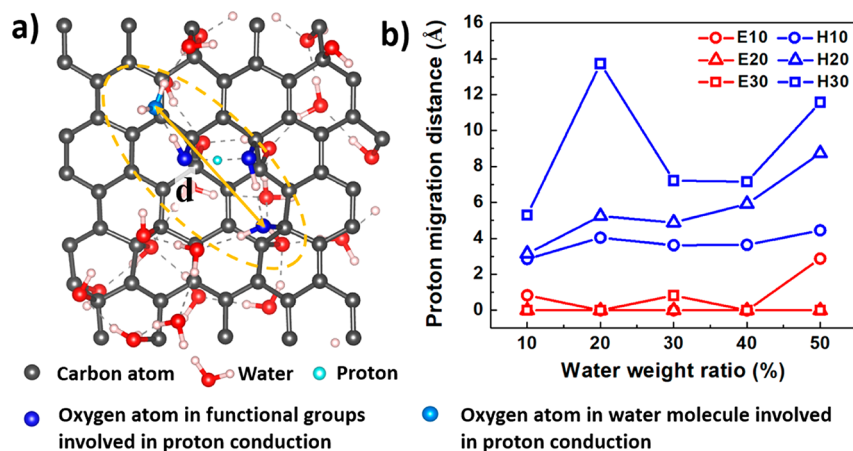

Figure 4. (a) Illustration of the proton migration distance. (b) Averaged proton migration distance for different GO sheets as a function of water weight ratio.

enough to induce a uniform distribution of adsorbed water molecules under these circumstances.

3.2. Proton Conduction Capability on the Surface of GO Sheets. To test the proton conduction capability of GO sheets with different kinds of functional groups, we introduced one extra proton into the prepared GO sheets with different amount of adsorbed water molecules. The extra proton was initially bonded with a randomly chosen epoxide or hydroxyl functional group. After a 100 ps ReaxFF MD simulation with the NVT ensemble ($T = 300$ K) for equilibration, we tracked the proton trajectories in another 1 ns ReaxFF MD simulation with the NVT ensemble ($T = 300$ K). During the 1 ns ReaxFF MD simulation, the relative position of adsorbed water molecules barely changes due to the strong hydrogen bonding, and a proton can hop among different oxygen atoms. As shown

in Figure 4, oxygen atoms involved in the proton conduction process during the 1 ns ReaxFF MD simulation were identified, and the longest distance between pairs of involved oxygen atoms was defined as the proton migration distance as shown in Figure 4a. The averaged proton migration distance for different GO sheets as a function of water weight ratio is shown in Figure 4b. We can see that for epoxide functional groups, the extra proton prefers to stick on one of the epoxide functional groups and barely move during the entire simulation time. For hydroxyl functional groups, the extra proton hops frequently, and the proton migration distance generally increases along with the number of functional groups and adsorbed water molecules. The proton-hopping data in both the cases of epoxide and hydroxyl functional groups are not

sufficient enough to calculate the mean-square displacement (MSD) and diffusivity.

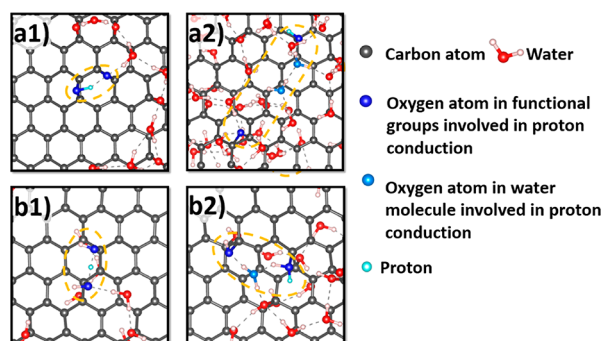We analyzed the proton migration trajectories and identified four proton-hopping modes, as shown in Figure 5. For GO

Figure 5. Illustration of four proton-hopping modes: (a1) proton hopping between adjacent epoxide functional groups, (a2) water-mediated proton hopping between nonadjacent epoxide functional groups, (b1) proton hopping between adjacent hydroxyl functional groups, and (b2) water-mediated proton hopping between non-adjacent hydroxyl functional groups.

sheets covered by epoxide functional groups, proton hopping between adjacent epoxide functional groups contributed most of the observed proton migration behavior. Only one case of water-mediated proton hopping between nonadjacent epoxide functional groups has been observed (see Figure 5a2). For GO sheets covered by hydroxyl functional groups, both proton hopping between adjacent hydroxyl functional groups and water-mediated proton hopping between nonadjacent hydroxyl functional groups can be observed. The water-mediated proton hopping between nonadjacent oxygen functional groups can result in a considerable proton migration distance and play a key role when GO serves as the proton conduction electrolyte.

3.3. Proton Conduction Energy Barriers on the Surface of GO Sheets. We quantitatively calculated the proton-hopping energy barriers on water-adsorbed GO sheets by analyzing the proton migration trajectories. As oxygen functional groups are unstable at high temperature,[10] accelerating proton motion by elevating simulation temperature[42,43] is impracticable. To collect enough proton-hopping data for further statistical analysis, we prepared smaller graphene sheets (1.97×1.71 nm^2) decorated by 20% epoxide or hydroxyl functional groups for long-time ReaxFF MD simulations. These GO sheets were put into a $1.97 \times 1.71 \times 2.50$ nm^3 cubic box containing 30 wt % water molecules, which agrees with most of the experimentally reported GO oxygen contents and humidity conditions.[16] Afterward, the systems went through 500 ps ReaxFF MD simulations in the NVT ensemble ($T = 300$ K) for equilibration. For both epoxide and hydroxyl GO sheets, 10 samples containing an extra proton with different initial proton positions were prepared. In five samples, the proton was randomly attached to one of the oxygen functional groups, while in the other five samples, the proton was randomly attached to one of the adsorbed water molecules. The prepared samples with the extra proton then went through a 100 ps ReaxFF MD simulation for equilibration in the NVT ensemble ($T = 300$ K). Afterward, production runs in the NVT ensemble ($T = 300$ K) were conducted.

The proton conduction behavior on the surface of GO sheets can be decomposed into four elementary proton-hopping processes, as illustrated in Figure 6: (a) proton
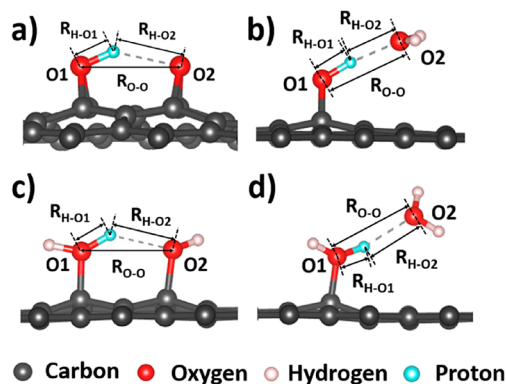

Figure 6. Illustration of four elementary proton-hopping processes between (a) adjacent epoxide functional groups, (b) epoxide functional group and adsorbed water molecule, (c) adjacent hydroxyl functional groups, and (d) hydroxyl functional group and adsorbed water molecule.

hopping between adjacent epoxide functional groups, (b) proton hopping between epoxide functional group and adsorbed water molecule, (c) proton hopping between adjacent hydroxyl functional groups, and (d) proton hopping between hydroxyl functional group and adsorbed water molecule. Proton transfer coordinate δ was defined as the distance difference between the proton and its two nearest oxygen atoms O1 and O2 ($\delta = R_{H-O1} - R_{H-O2}$).[44,45] R_{O-O} was defined as the distance between O1 and O2 atoms. For each frame in the production runs, the δ and R_{O-O} values were calculated, and the energy barrier was calculated as

$$\Delta F = -k_B T \ln P \tag{4}$$

where k_B is the Boltzmann constant, T is the temperature, and P is the probability as a function of proton transfer coordinate δ. For the case of both epoxide and hydroxyl functional groups, the 10 trajectories with different initial proton positions were analyzed every 500 ps until the energy profiles reached a convergence criterion of 0.005 eV.

The resulted energy profiles for proton conduction on GO sheets containing epoxide functional groups can be found in Figure 7, and the results for convergence tests can be found in Figures S13 and S14. As shown in Figure 7a, proton hopping between adjacent epoxide functional groups exhibits a moderate energy barrier of 0.212 eV, which explains the observed unfrequent proton hopping in Figure 4b. Proton hopping between epoxide functional group and adsorbed water molecule is much harder. Compared with forming a hydronium ion, being adsorbed on epoxide functional groups is a much more stable state. During the 11.5 ns ReaxFF MD simulations of 10 cases with different initial proton positions, no δ value falls into the range between -0.025 and 0.025 Å (highlighted by the light blue color in Figure 7b1). Thus, the free energy barrier for proton hopping between the epoxide functional group and an adsorbed water molecule is expected to be higher than 0.422 eV, which can barely occur at room temperature. Therefore, water-mediated long-range proton conduction between nonadjacent epoxide functional groups is very difficult to happen spontaneously, which is also consistent with our previous observations.
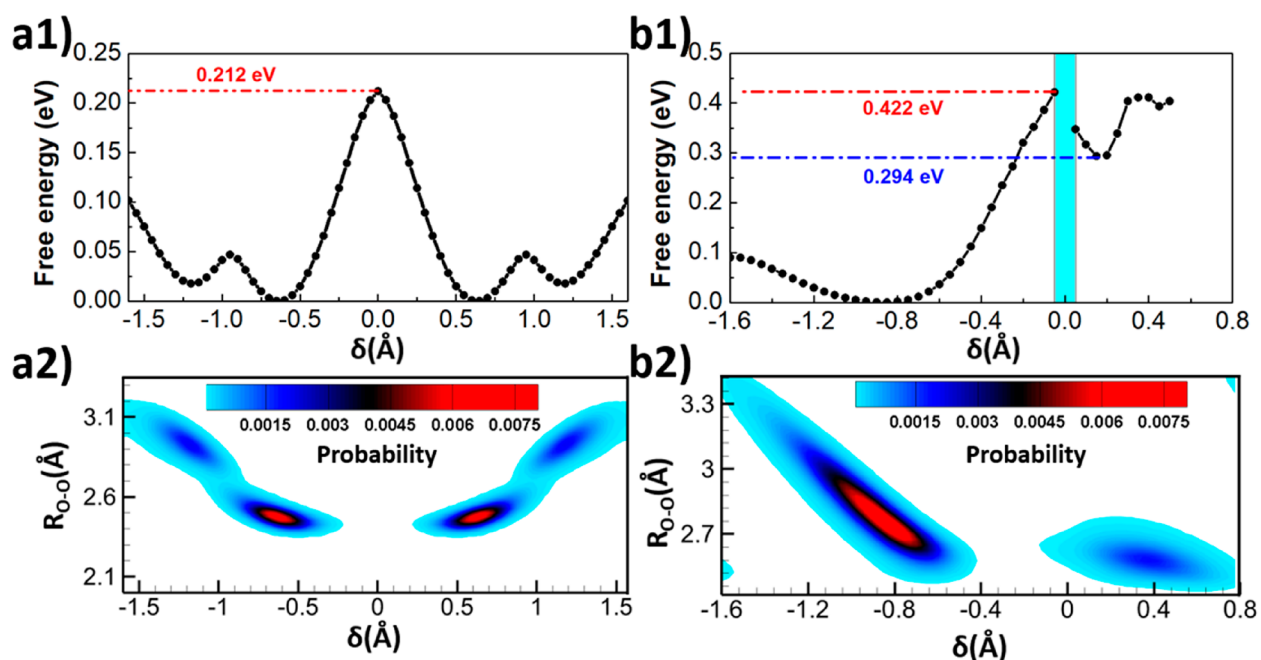
Figure 7. (a1) Free energy profile and (a2) probability distribution of proton as a function of δ and R_{O-O} for proton hopping between adjacent epoxide functional groups. (b1) Free energy profile and (b2) probability distribution of proton as a function of δ and R_{O-O} for proton hopping between epoxide functional group and adsorbed water molecule.
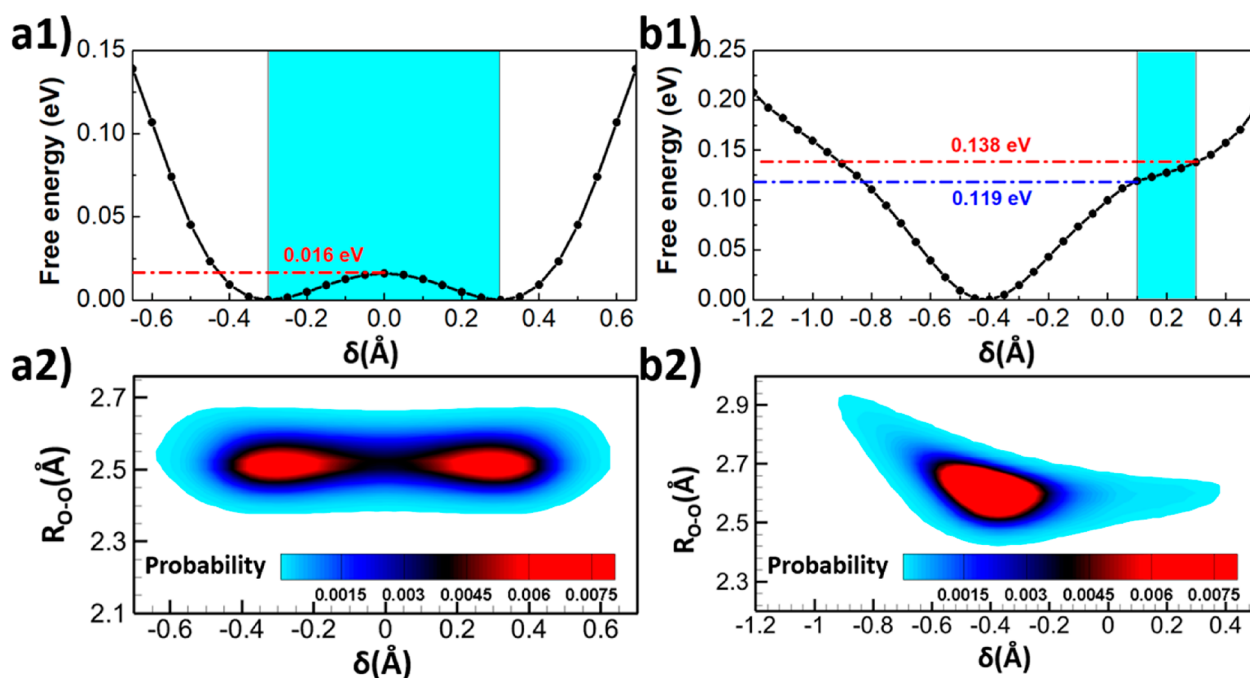

Figure 8. (a1) Free energy profile and (a2) probability distribution of proton as a function of δ and R_{O-O} for proton hopping between adjacent hydroxyl functional groups. (b1) Free energy profile and (b2) probability distribution of proton as a function of δ and R_{O-O} for proton hopping between the hydroxyl functional group and adsorbed water molecule.

The energy profiles for proton conduction on the surface of GO sheets containing hydroxyl functional groups can be found in Figure 8 (results for convergence tests can be found in Figures S15 and S16). As shown in Figure 8a, the energy barrier for proton hopping between adjacent hydroxyl functional groups is as low as 0.016 eV, which can be regarded as barrierless at room temperature and agrees well with the previously reported proton conduction capability of hydroxyl-functionalized graphane.[42,43] The energy profile for proton

hopping between the hydroxyl functional group and adsorbed water molecule can be found in Figure 8b. Similar to the case of epoxide functional groups, a proton prefers to attach to a hydroxyl functional group rather than combine with an adsorbed water molecule to form a hydronium ion. When the δ value falls into the range between 0.1 and 0.3 Å, a hydronium ion can be formed, which corresponds to the plateau area highlighted by the light blue color in Figure 8b1. Under this circumstance, the proton in the hydronium ion can

be further passed to another neighboring hydroxyl functional group or water molecule to accomplish the water-mediated proton conduction. The energy barrier for proton hopping between hydroxyl functional group and adsorbed water molecule is estimated to be 0.119−0.138 eV, which is much lower than the case of epoxide functional groups and can contribute to a good proton conductivity. The presence of adsorbed water molecules bridges nonadjacent hydroxyl functional groups and makes long-range proton conduction possible at a relatively low hydroxyl content.

4. CONCLUSIONS

We performed extensive ReaxFF MD simulations to investigate the detailed water-mediated proton conduction mechanism along the surface of GO sheets. We found that both epoxide and hydroxyl functional groups can effectively attract water molecules onto the surface of GO sheets and form a hydrogen-bonding network. Twenty weight percent of oxygen functional groups are enough to induce a relatively homogeneous distribution of adsorbed water molecules. Instead of bonding with adsorbed water molecules to form hydronium ions, protons prefer to bond with oxygen functional groups on the surface of GO sheets. Proton conduction on the surface of GO sheets covered by pure epoxide functional groups can barely occur for the relatively high energy barriers. On the other hand, proton hopping between adjacent hydroxyl functional groups is almost barrierless. The energy barrier for water-mediated proton conduction between nonadjacent hydroxyl functional groups is estimated to be 0.119−0.138 eV, which is also feasible at room temperature. The adsorbed water molecules provide bridges for proton conduction between nonadjacent hydroxyl functional groups and can contribute to a good proton conductivity. Our work clarified the water-mediated proton conduction mechanism of GO sheets and shed light on the future design of GO-based proton conductors.

■ ASSOCIATED CONTENT

Ⓢ Supporting Information

The Supporting Information is available free of charge at https://pubs.acs.org/doi/10.1021/acs.chemmater.0c01512.

> GO model preparation process; water adsorption behavior on the surface of graphene oxide; convergence tests for energy profiles; relationship between water weight ratio and relative humidity (PDF)

■ AUTHOR INFORMATION

Corresponding Author

Le Shi − State Key Laboratory of Electrical Insulation and Power Equipment, Center of Nanomaterials for Renewable Energy, School of Electrical Engineering, Xi'an Jiaotong University, Xi'an 710049, China; ⓞ orcid.org/0000-0003-1468-4549; Email: le.shi@mail.xjtu.edu.cn

Authors

Zhixuan Ying − State Key Laboratory of Electrical Insulation and Power Equipment, Center of Nanomaterials for Renewable Energy, School of Electrical Engineering, Xi'an Jiaotong University, Xi'an 710049, China

Ao Xu − School of Aeronautics, Northwestern Polytechnical University, Xi'an 710072, China

Yonghong Cheng − State Key Laboratory of Electrical Insulation and Power Equipment, Center of Nanomaterials for Renewable Energy, School of Electrical Engineering, Xi'an Jiaotong University, Xi'an 710049, China

Complete contact information is available at:
https://pubs.acs.org/10.1021/acs.chemmater.0c01512

Author Contributions

L.S. conceived the research and designed the numerical simulations; L.S., Z.Y., and A.X. analyzed the data; L.S. wrote the paper; L.S., Z.Y., A.X., and Y.C. discussed the manuscript.

Notes

The authors declare no competing financial interest.

■ REFERENCES

(1) Yang, Y.; Yang, X.; Liang, L.; Gao, Y.; Cheng, H.; Li, X.; Zou, M.; Ma, R.; Yuan, Q.; Duan, X. Large-Area Graphene-Nanomesh/Carbon-Nanotube Hybrid Membranes for Ionic and Molecular Nanofiltration. Science 2019, 364, 1057−1062.

(2) Surwade, S. P.; Smirnov, S. N.; Vlassiouk, I. V.; Unocic, R. R.; Veith, G. M.; Dai, S.; Mahurin, S. M. Water Desalination Using Nanoporous Single-Layer Graphene. Nat. Nanotechnol. 2015, 10, 459−464.

(3) Shi, L.; Xu, A.; Cheng, Y. H. Ether-Group-Mediated Aqueous Proton Selective Transfer Across Graphene-Embedded 18-Crown-6 Ether Pores. J. Phys. Chem. C 2019, 123, 27429−27435.

(4) Hu, S.; Lozada-Hidalgo, M.; Wang, F. C.; Mishchenko, A.; Schedin, F.; Nair, R. R.; Hill, E. W.; Boukhvalov, D. W.; Katsnelson, M. I.; Dryfe, R. A.; Grigorieva, I. V.; Wu, H. A.; Geim, A. K. Proton Transport Through One-Atom-Thick Crystals. Nature 2014, 516, 227−230.

(5) Shi, L.; Xu, A.; Pan, D.; Zhao, T. S. Aqueous Proton-Selective Conduction Across Two-Dimensional Graphyne. Nat. Commun. 2019, 10, 1−8.

(6) Shi, L.; Xu, A.; Chen, G.; Zhao, T. S. Theoretical Understanding of Mechanisms of Proton Exchange Membranes Made of 2D Crystals with Ultrahigh Selectivity. J. Phys. Chem. Lett. 2017, 8, 4354−4361.

(7) Mi, B. Graphene Oxide Membranes for Ionic and Molecular Sieving. Science 2014, 343, 740−742.

(8) Ries, L.; Petit, E.; Michel, T.; Diogo, C. C.; Gervais, C.; Salameh, C.; Bechelany, M.; Balme, S.; Miele, P.; Onofrio, N.; Voiry, D. Enhanced Sieving from Exfoliated MoS2Membranes via Covalent Functionalization. Nat. Mater. 2019, 18, 1112−1117.

(9) Raidongia, K.; Huang, J. Nanofluidic Ion Transport Through Reconstructed Layered Materials. J. Am. Chem. Soc. 2012, 134, 16528−16531.

(10) Dreyer, D. R.; Park, S.; Bielawski, C. W.; Ruoff, R. S. The Chemistry of Graphene Oxide. Chem. Soc. Rev. 2010, 39, 228−240.

(11) Joshi, R. K.; Carbone, P.; Wang, F. C.; Kravets, V. G.; Su, Y.; Grigorieva, I. V.; Wu, H. A.; Geim, A. K.; Nair, R. R. Precise and Ultrafast Molecular Sieving Through Graphene Oxide Membranes. Science 2014, 343, 752−754.

(12) Zhou, K. G.; Vasu, K. S.; Cherian, C. T.; Neek-Amal, M.; Zhang, J. C.; Ghorbanfekr-Kalashami, H.; Huang, K.; Marshall, O. P.;

Kravets, V. G.; Abraham, J.; et al. Electrically Controlled Water Permeation Through Graphene Oxide Membranes. *Nature* **2018**, *559*, 236−240.

(13) Zhang, M.; Mao, Y.; Liu, G.; Liu, G.; Fan, Y.; Jin, W. Molecular Bridges Stabilize Graphene Oxide Membranes in Water. *Angew. Chem., Int. Ed.* **2020**, *59*, 1689−1695.

(14) Chen, L.; Shi, G.; Shen, J.; Peng, B.; Zhang, B.; Wang, Y.; Bian, F.; Wang, J.; Li, D.; Qian, Z.; et al. Ion Sieving in Graphene Oxide Membranes via Cationic Control of Interlayer Spacing. *Nature* **2017**, *550*, 380−383.

(15) Karim, M. R.; Hatakeyama, K.; Matsui, T.; Takehira, H.; Taniguchi, T.; Koinuma, M.; Matsumoto, Y.; Akutagawa, T.; Nakamura, T.; Noro, S. I.; et al. Graphene Oxide Nanosheet with High Proton Conductivity. *J. Am. Chem. Soc.* **2013**, *135*, 8097−8100.

(16) Pandey, R. P.; Shukla, G.; Manohar, M.; Shahi, V. K. Graphene Oxide Based Nanohybrid Proton Exchange Membranes for Fuel Cell Applications: An Overview. *Adv. Colloid Interface Sci.* **2017**, *240*, 15−30.

(17) Gao, W.; Wu, G.; Janicke, M. T.; Cullen, D. A.; Mukundan, R.; Baldwin, J. K.; Brosha, E. L.; Galande, C.; Ajayan, P. M.; More, K. L.; et al. Ozonated Graphene Oxide Film as a Proton-Exchange Membrane. *Angew. Chem., Int. Ed.* **2014**, *53*, 3588−3593.

(18) Wang, L. S.; Lai, A. N.; Lin, C. X.; Zhang, Q. G.; Zhu, A. M.; Liu, Q. L. Orderly Sandwich-Shaped Graphene Oxide/Nafion Composite Membranes for Direct Methanol Fuel Cells. *J. Membr. Sci.* **2015**, *492*, 58−66.

(19) Kida, T.; Kuwaki, Y.; Miyamoto, A.; Hamidah, N. L.; Hatakeyama, K.; Quitain, A. T.; Sasaki, M.; Urakawa, A. Water Vapor Electrolysis with Proton-Conducting Graphene Oxide Nanosheets. *ACS Sustainable Chem. Eng.* **2018**, *6*, 11753−11758.

(20) Gao, W.; Singh, N.; Song, L.; Liu, Z.; Reddy, A. L.; Ci, L.; Vajtai, R.; Zhang, Q.; Wei, B.; Ajayan, P. M. Direct Laser Writing of Micro-Supercapacitors on Hydrated Graphite Oxide Films. *Nat. Nanotechnol.* **2011**, *6*, 496.

(21) Cao, L.; Wu, H.; Yang, P.; He, X.; Li, J.; Li, Y.; Xu, M.; Qiu, M.; Jiang, Z. Graphene Oxide-Based Solid Electrolytes with 3D Prepercolating Pathways for Efficient Proton Transport. *Adv. Funct. Mater.* **2018**, *28*, 1804944.

(22) Simari, C.; Stallworth, P.; Peng, J.; Coppola, L.; Greenbaum, S.; Nicotera, I. Graphene Oxide and Sulfonated-Derivative: Proton Transport Properties and Electrochemical Behavior of Nafion-Based Nanocomposites. *Electrochim. Acta* **2019**, *297*, 240−249.

(23) Meng, Q. L.; Liu, H. C.; Huang, Z.; Kong, S.; Lu, X.; Tomkins, P.; Jiang, P.; Bao, X. Mixed Conduction Properties of Pristine Bulk Graphene Oxide. *Carbon* **2016**, *101*, 338−344.

(24) Singh, C.; Nikhil, S.; Jana, A.; Mishra, A. K.; Paul, A. Proton Conduction Through Oxygen Functionalized Few-Layer Graphene. *Chem. Commun.* **2016**, *52*, 12661−12664.

(25) Hatakeyama, K.; Karim, M. R.; Ogata, C.; Tateishi, H.; Funatsu, A.; Taniguchi, T.; Koinuma, M.; Hayami, S.; Matsumoto, Y. Proton Conductivities of Graphene Oxide Nanosheets: Single, Multilayer, and Modified Nanosheets. *Angew. Chem., Int. Ed.* **2014**, *53*, 6997−7000.

(26) Wu, L.; Jiang, X. Proton Transfer at the Interaction Interface of Graphene Oxide. *Anal. Chem.* **2018**, *90*, 10223−10230.

(27) Dong, D.; Zhang, W.; van Duin, A. C.; Bedrov, D. Grotthuss Versus Vehicular Transport of Hydroxide in Anion-Exchange Membranes: Insight from Combined Reactive and Nonreactive Molecular Simulations. *J. Phys. Chem. Lett.* **2018**, *9*, 825−829.

(28) Zhang, W.; Dong, D.; Bedrov, D.; van Duin, A. C. Hydroxide Transport and Chemical Degradation in Anion Exchange Membranes: A Combined Reactive and Non-Reactive Molecular Simulation Study. *J. Mater. Chem. A* **2019**, *7*, 5442−5452.

(29) Lin, L. C.; Grossman, J. C. Atomistic Understandings of Reduced Graphene Oxide as an Ultrathin-Film Nanoporous Membrane for Separations. *Nat. Commun.* **2015**, *6*, 1−7.

(30) Zhang, W.; van Duin, A. C. Improvement of the ReaxFF Description for Functionalized Hydrocarbon/Water Weak Inter-

actions in the Condensed Phase. *J. Phys. Chem. B* **2018**, *122*, 4083−4092.

(31) Zhang, W.; Chen, X.; van Duin, A. C. Isotope Effects in Water: Differences of Structure, Dynamics, Spectrum, and Proton Transport Between Heavy and Light Water from ReaxFF Reactive Force Field Simulations. *J. Phys. Chem. Lett.* **2018**, *9*, 5445−5452.

(32) Plimpton, S. Fast Parallel Algorithms for Short-Range Molecular Dynamics. *J. Comput. Phys.* **1995**, *117*, 1−9.

(33) Aktulga, H. M.; Fogarty, J. C.; Pandit, S. A.; Grama, A. Y. Parallel Reactive Molecular Dynamics: Numerical Methods and Algorithmic Techniques. *Parallel Comput.* **2012**, *38*, 245−259.

(34) de Aquino, B. R.; Ghorbanfekr-Kalashami, H.; Neek-Amal, M.; Peeters, F. M. Ionized Water Confined in Graphene Nanochannels. *Phys. Chem. Chem. Phys.* **2019**, *21*, 9285−9295.

(35) Shi, L.; Ying, Z. X.; Xu, A.; Cheng, Y. H. Anomalous Proton Conduction Behavior Across Nanoporous Two-Dimensional Conjugated Aromatic Polymer Membrane. *Phys. Chem. Chem. Phys.* **2020**, *22*, 2978−2985.

(36) Erickson, K.; Erni, R.; Lee, Z.; Alem, N.; Gannett, W.; Zettl, A. Determination of the Local Chemical Structure of Graphene Oxide and Reduced Graphene Oxide. *Adv. Mater.* **2010**, *22*, 4467−4472.

(37) Williams, C. D.; Carbone, P.; Siperstein, F. R. In Silico Design and Characterization of Graphene Oxide Membranes with Variable Water Content and Flake Oxygen Content. *ACS Nano* **2019**, *13*, 2995−3004.

(38) Korobov, M. V.; Talyzin, A. V.; Rebrikova, A. T.; Shilayeva, E. A.; Avramenko, N. V.; Gagarin, A. N.; Ferapontov, N. B. Sorption of Polar Organic Solvents and Water by Graphite Oxide: Thermodynamic Approach. *Carbon* **2016**, *102*, 297−303.

(39) Taherian, F.; Marcon, V.; van der Vegt, N. F.; Leroy, F. What is the Contact Angle of Water on Graphene? *Langmuir* **2013**, *29*, 1457−1465.

(40) Tocci, G.; Joly, L.; Michaelides, A. Friction of Water on Graphene and Hexagonal Boron Nitride From Ab Initio Methods: Very Different Slippage Despite Very Similar Interface Structures. *Nano Lett.* **2014**, *14*, 6872−6827.

(41) Ruiz-Barragan, S.; Muñoz-Santiburcio, D.; Marx, D. Nanoconfined Water Within Graphene Slit Pores Adopts Distinct Confinement-Dependent Regimes. *J. Phys. Chem. Lett.* **2019**, *10*, 329−334.

(42) Bagusetty, A.; Choudhury, P.; Saidi, W. A.; Derksen, B.; Gatto, E.; Johnson, J. K. Facile Anhydrous Proton Transport on Hydroxyl Functionalized Graphane. *Phys. Rev. Lett.* **2017**, *118*, 186101.

(43) Bagusetty, A.; Johnson, J. K. Unraveling Anhydrous Proton Conduction in Hydroxygraphane. *J. Phys. Chem. Lett.* **2019**, *10*, 518−523.

(44) Xu, J.; Jiang, H.; Shen, Y.; Li, X. Z.; Wang, E. G.; Meng, S. Transparent Proton Transport Through a Two-Dimensional Nanomesh Material. *Nat. Commun.* **2019**, *10*, 1−8.

(45) Pan, D.; Galli, G. The Fate of Carbon Dioxide in Water-Rich Fluids Under Extreme Conditions. *Sci. Adv.* **2016**, *2*, e1601278.